The Paleoproterozoic and Neoproterozoic Carbon Cycle Promoted the Evolution of a Habitable Earth

LIU Zhicheng and ZHANG Lifei*

Key Laboratory of Orogenic Belt and Crustal Evolution, Ministry of Education, School of Earth and Space Sciences, Peking University, Beijing 100871, China

Abstract: The carbon cycle is an important process that regulates Earth's evolution. We compare two typical periods, in the Paleoproterozoic and Neoproterozoic, in which many geological events occurred. It remains an open question when modern plate tectonics started on Earth and how it has influenced the carbon cycle through time. In the Paleoproterozoic, intense weathering in a highly CO_2 and CH_4 rich atmosphere caused more nutritional elements to be carried into the ocean. Terrestrial input boosted high biological productivity, deposition of sediments and the formation of an altered oceanic crust, which may have promoted an increase in the oxygen content. Sediment lubrication and a decrease in mantle potential temperature made cold and deep subduction possible, which carried more carbon into the deep mantle. Carbon can be stored in the mantle as diamond and carbonated mantle rocks, being released by arc and mid-ocean ridge outgassing at widely different times. From the Paleoproterozoic through the Neoproterozoic to the Phanerozoic, the carbon cycle has promoted the evolution of a habitable Earth.

Key words: carbon cycle, great oxidation event, modern subduction, Paleoproterozoic, Neoproterozoic

Citation: Liu and Zhang, 2023. The Paleoproterozoic and Neoproterozoic Carbon Cycle Promoted the Evolution of a Habitable Earth. Acta Geologica Sinica (English Edition), 97(1): 316–326. DOI: 10.1111/1755-6724.15046

1 Introduction

Carbon plays a significant role in the development of the Earth system. Carbon not only participates in the construction of the biosphere as the most basic element of life, but also influences Earth's evolution. In the atmosphere, the content of CO_2 and CH_4 has affected global climate change throughout Earth's history. Being an important agent for carbonatite metasomatism, it influences the lithospheric mantle oxygen fugacity through deep subduction and forms carbon reservoirs at different depths in the form of diamonds and other carbon-bearing rocks, causing mantle heterogeneity (Dasgupta and Hirschmann, 2010). The carbonated mantle at different depths has reciprocally produced various magmas (basalt magma, carbonatite magma, etc.) during different geological periods, slowly releasing the carbon which was previously stored in the deep mantle, thus affecting the carbon content of surface-atmosphere composition and cycling over a protracted period (Penman et al., 2020). Therefore, by studying the carbon cycle, we can explore how Earth's surface and the deep earth have interacted during important geological events, thus profoundly influencing the interaction and co-evolutionary process between the realms of Earth's surface and the deep earth.

The diversity of carbon forms can be represented in gas, liquid and solid phases of carbon in different spheres (CO_2 and CH_4 in the atmosphere, carbon-based organic matter in the biosphere, carbonate, carbonate ion in the hydrosphere and carbonatite magma, diamond, carbonated peridotite in the mantle, etc.) and their respective special isotopic compositions during Earth's material cycle. However, the exchange of materials and energy between different reservoirs and spheres can be reflected through the changes in carbon phases and geochemical properties. With the exception of carbon, other elements with high abundance on Earth do not exhibit these characteristics, such as potassium, sodium, calcium, magnesium, iron, aluminum, phosphorus, silicon, nitrogen, and so on. As hydrogen, oxygen, and nitrogen cannot exist as typical rocks in the deep earth, it is challenging to identify their possible sources in Earth's deep parts. Furthermore, with the exception of carbon, the deep mantle has no independent huge reservoir reflecting these characteristics of the elements, making it difficult to define their migratory processes. Therefore, carbon is the best information carrier for earth's material cycle. This process is also reflected in Earth's surface environment as CO_2 is exhausted from the atmosphere to solution ions in the form of CO_3^{2-} and HCO_3^-, then flows into the sea with surface runoff. In the ocean, the terrestrial weathering materials enriched with C, Fe, Na, P, Mg and other biological nutrient elements promote biological reproduction and carbon fixation of marine organisms, which resulting in the deposition of organic carbon and carbonate rocks on the ocean floor (Ganade De Araujo et al., 2014). Simultaneously, the elevated contents of K^+, Na^+, CO_3^{2-} and HCO_3^- in the ocean also promote the weathering of the ocean floor, forming carbonated basalt and peridotite. During subduction, these carbon-rich

* Corresponding author. E-mail: lfzhang@pku.edu.cn

materials deposited on the ocean floor can be released and either re-fixed at different depths of the subduction zone, or subducted into the deep mantle (Plank and Manning, 2019). In the shallow part of the subduction zone, due to changes in temperature and pressure, partially-consolidated carbon re-enters the atmosphere through decarbonation processes such as dissolution and melting, as with metamorphism and island arc magmatism, regulating the greenhouse gas content of the atmosphere and affecting Earth's surface temperature (McKenzie et al., 2016). The changes in Earth's surface temperature reciprocally promotes or suppresses the weathering process. In the deep mantle, the overlying mantle lithosphere is metasomatized by carbon-rich melts and fluids formed by the dissolving and melting of subducting plates and the carbonatite metasomatic lithospheric mantle is transformed into a huge sink storing large amounts of carbon (Tappe et al., 2017). This transformed carbon-bearing mantle is also a source of atmospheric CO_2 via intraplate volcanism over a longer time scale than from shallow decarbonation. Thus, climate change on a global scale is profoundly affected by the deep carbon cycle.

The atmosphere of the early Earth (>2.5 Ga) was full of carbon-rich gases such as CO_2 and CH_4 (Pavlov et al., 2000), rather than an atmosphere dominated by nitrogen and oxygen, as in the Phanerozoic eon. The early process of carbon being removed from the atmosphere and entering the mantle for sequestration has profoundly affected the evolution of both the atmosphere and of Earth's interior. The starting time and operating mechanism of this process is still unconstrained. However, the modern plate subduction mechanisms can effectively make carbon-bearing materials to be subducted into the deep mantle to complete the carbon cycle on different sphere time scales (Dasgupta and Hirschmann, 2010). Whether or not carbon can be transported to Earth's depths by plate subduction has been a research topic explored by geologists for decades. In fact, under the 'thermal subduction' system of high-temperature gradients, carbon-rich rocks in the shallow subduction zone undergo decarbonation and carbon release, so it is difficult for carbon to enter the deep parts of the earth. Therefore, only a 'cold subduction' mechanism, similar to the current form of plate subduction, could send carbon-rich materials into the deep earth (Dasgupta and Hirschmann, 2010). Recent studies have shown that the current form of global plate subduction first appeared in the early Paleoproterozoic (Xu et al., 2018; Li et al., 2023). Thus, when and how carbon uptake from the atmosphere was first subducted into the deep mantle and how the carbon cycle coupled with the evolution of a habitable Earth, are under debate. This paper reviews through summarizing the interactive relationships amongst the carbon cycle, oxidation events and modern plate subduction, in order to stress the important role of the carbon cycle in promoting the habitable evolution of Earth.

2 The Coupling of the Carbon Cycle and Oxidation Events

The great oxidation event (GOE) is a geological event that has attracted much attention in the past 20 years. Earth's surface-atmosphere was anoxic in Archaean and older periods, until 2.4–2.3 Ga, when the oxygen content increased significantly (Lyons et al., 2014). The change of oxygen in the atmosphere can be fully reflected in the mass-independent fractionation of sulfur isotopes (S-MIF) in sedimentary rocks. Before the great oxidation event, the atmosphere lacked an ozone layer, thus sedimentary rocks were produced with abnormally large $\delta^{33}S$ deposits. Indeed, the generation and preservation of this $\delta^{33}S$ anomaly (S-MIF signal) required a very low atmospheric oxygen concentration (Farquhar et al., 2000). In the <2.2 Ga sedimentary rocks, the disappearance of the S-MIF and the increase of variable valence elements such as U and Mo indicates that the concentration of oxygen in the atmosphere at that time increased significantly, even exceeding 10% of the current atmospheric oxygen level (Luo et al., 2016). However, in the Mesoproterozoic, the oxygen concentration decreased rapidly, although it was not low enough for the $\delta^{33}S$ anomaly to be detectable. Some redox-sensitive elements such as U, Cr and Mo in shale show that the atmospheric oxygen content at this time had decreased to a greater extent than that before the great oxidation event and remained stable at this level for a long time. In the Neoproterozoic, the oxygen concentration in the atmosphere again significantly increased and reached the level of 10%–50% of the current levels, which represents the second Earth oxidation event, the 'Neoproterozoic oxidation event', when oxidation appeared in the deep-sea for the first time (Alcott et al., 2019). Geologists have given different explanations for the origin of oxygen. Some reseachers believe that hydrogen produced by the photolysis of water and methane escaped into outer space, resulting in the gradual oxidation of Earth's atmosphere (Lehmer et al., 2020). Others found through high temperature and high-pressure tests that partial melting of the FeO_2 accumulated at the core-mantle boundary might have promoted the oxidation of the surface and the GOE (Hu et al., 2016). Some studies found a discontinuity of geochemical elements in the 2.5 Ga period. The Fe in tonalite-trondhjemite-granodiorite (TTG) formed by partial melting of sodium clinopyroxene and garnet prior to 2.5 Ga was controlled by the distribution coefficient and had a low Fe^{3+}/Fe^{2+} content, which made it balanced with the reducing gas and hindered the oxidation of the atmosphere until TTG was no longer generated after 2.5 Ga (Keller and Schoene, 2012). Some researchers concluded that the increase of terrestrial volcanoes at 2.5 Ga and the decrease of ocean floor volcanoes and their reducing gases promoted the increase of oxygen composition in the atmosphere (Kump and Barley, 2007). Studies also indicated that the transformation of the 3.0–2.5 Ga continental composition from mafic to felsic reduced the oxidation rate of the surface and was conducive to the accumulation of oxygen. From Paleoproterozoic to Neoproterozoic, the release of the continental carbon sink over the past billion years has promoted weathering and burial of organic carbon, resulting in the second increase of oxygen content (Lee et al., 2016). The transformation of continental composition has also led to a significant reduction in the flux of Ni into the ocean. Ni is an essential element for methanogens. The lack of Ni in the ocean has reduced the rate of microbial methane production, leading to the increase in oxygen (Konhauser et al., 2009). However, these explanations cannot find a common link between the GOE (Paleoproterozoic) and the NOE (Neoproterozoic) which have many similarities.

The rise in oxygen requires not only the increases of oxygen but also burial of the reducing substances. Intense weathering consumed CO_2 and brought nutrient elements of life such as C, P, Mg, Fe, K and so forth, into the ocean, which promoted oxygen production and cyanobacteria reproduction. The Lomagundi event, marked by a carbonate positive δ^{13}C excursion, indicates massive burial of organic carbon. Furthermore, weathering products increased the burial of organic carbon, which led to the net accumulation of oxygen (Campbell and Allen, 2008). Experimental petrology shows that organic carbon might be graphitized in the subduction zone without decarburization, thus allowing it to be carried into the deep mantle, facilitating the rise and maintenance of atmospheric oxygen (Duncan and Dasgupta, 2017; Eguchi et al., 2020). Organic carbon subducted into the deep mantle maintained a high oxygen content longer than burial in the crust, causing the 'boring billion' to maintain a higher oxygen content than before the GOE. Especially in the Phanerozoic, organic carbon was subducted into the deep mantle by the modern subduction system, helping to maintain an oxidizing atmosphere. The periods of weathering were consistent with the oxidation events (Fig. 1). Thus, both the Paleoproterozoic and Neoproterozoic had intense weathering, oxidation events and a positive δ^{13}C excursion, which imply a coupling effect between the carbon cycle and the oxygen cycle.

3 Carbon Subducted into the Deep Mantle by Modern Subduction

At present, metamorphic rocks formed in the Archean with high pressure and low temperature (<500 °C/GPa) relating to subduction and collision have not been found, but high pressure and ultra-high pressure rocks have been found all over the world in many Paleoproterozoic orogenic belts related to the formation of the Columbia supercontinent (Brown et al., 2020). Eclogite with oceanic crust characteristics was found in the 2.0 Ga Usagaran orogenic belt and the 1.8 Ga Ubendian orogenic belt, Tanzania (Boniface et al., 2012). The eclogites found in the Eburnian Transamazonian orogenic belt in the Democratic Republic of Congo were produced in mafic rocks that underwent high-pressure and low-temperature conditions at 2.0 Ga (François et al., 2018; Loose and Schenk, 2018). Eclogites from the Kola Lapland orogenic belt of Russia, the Nagssugtoqidian orogenic belt of southeastern Greenland, the trans-Hudson orogenic belt of North America, the snowbird structural belt of Canada and the Central Orogenic Belt of the North China Craton have a similar age of 1.9 Ga (Moller et al., 1995; Baldwin et al., 2004; Ganne et al., 2012; Glassley et al., 2014; Weller and St-Onge, 2017; Yu et al., 2017; Müller et al., 2018; Xu et al., 2018; Zhang et al., 2020). Seismic and paleomagnetic evidence from six continents have revealed that the earliest global plate movements occurred at 2.0 Ga (Wan et al., 2020). Study of Paleoproterozoic orogenic belts and metamorphic rocks indicates that there are obvious concentrations in the occurrence of low-temperature and high-pressure metamorphic rocks in different orogenic belts at 2.1–1.8 Ga (Fig. 2). The study of mantle potential temperature showed that the temperature of the mantle

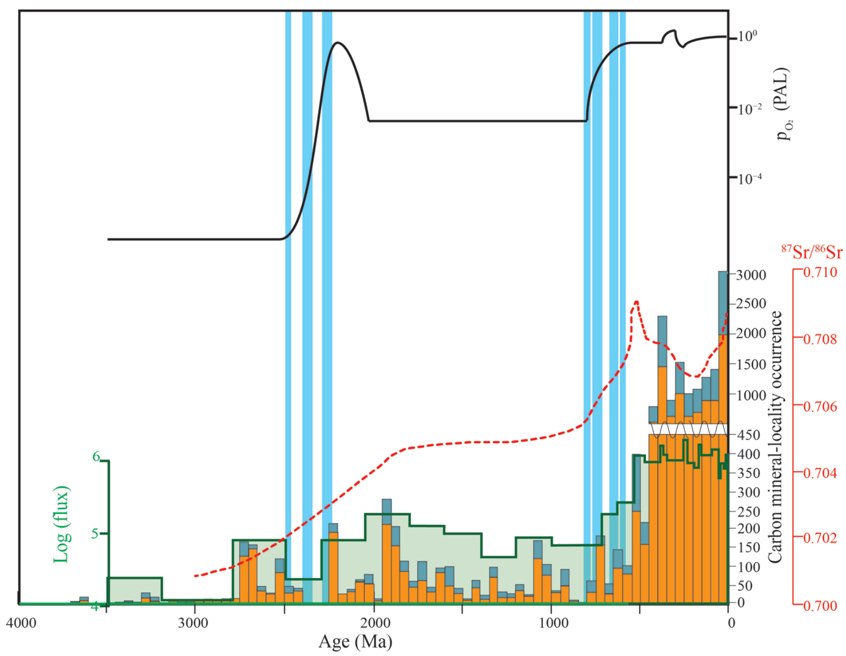

Fig. 1. Oxygen content (Lyons et al., 2014), Sr isotope and carbon-bearing sediments.

The black line represents the oxygen content of the atmosphere. The blue bars represents ice ages. The red dashed line shows Sr isotopes of carbonates in geological history and indicates weathering intensity (Shields and Veizer, 2002). The green shadows represent sediment flux. Orange bars and grey-blue bars represent the mineral-locality occurrence of anhydrous carbonates and hydrous carbonates, respectively (Husson and Peters, 2017; Hazen et al., 2019).

increased slowly from Earth's formation until Earth's temperature began to decrease slowly in the early Archean (Herzberg et al., 2010). Although the mantle potential temperature in the late Archean was about only 100°C higher than at 2.0 Ga, the lithosphere was thin because the continental crust was still in the early stage of thickening (Dhuime et al., 2015) and the *T*/*P* was high. Before the late Archean, the subduction plate and its plate-carried sediment experienced a high degree of melting under the hot mantle's potential temperature, so it was difficult to carry out continuous subduction to the deep mantle (Palin et al., 2020). In the period of the Paleoproterozoic orogenic belt (2.0–1.8 Ga), the continental crust had sufficient thickness and multiple cratons were formed (Perchuk et al., 2020). With the continuous reduction of

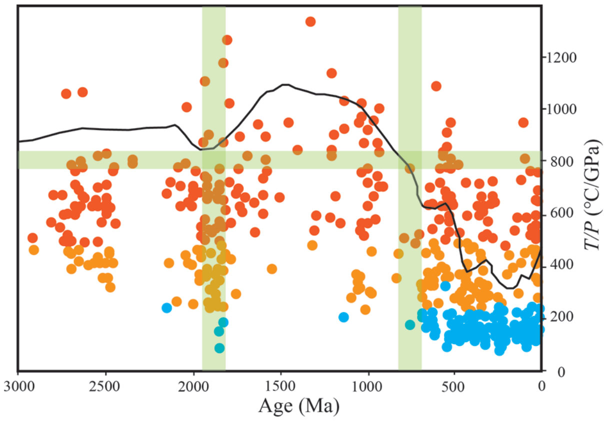

Fig. 2. Temperature and pressure of metamorphic rocks in geological history (Brown and Johnson, 2018; Brown et al., 2020).

Blue dots represent low *T*/*P* eclogite and orange dots and red dots represent middle and high *T*/*P* rocks like granulite or amphibolite. The black line represents the mean *T*/*P* of metamorphic rock. Green bars represent the *T*/*P* of the Paleoproterozoic and Neoproterozoic cold subduction of around 800 °C/GPa in these periods.

mantle potential temperature, the global metamorphic *T*/*P* ratio decreased significantly (Holder et al., 2019; Brown et al., 2020). The 2.0 Ga global metamorphic *T*/*P* ratio is equivalent to and approaches the 0.8 Ga metamorphic temperature pressure ratio (Fig. 2). At 0.8 Ga, a large number of typical cold, deep subduction rock assemblages, such as blueschists and ultra-high pressure metamorphic rocks, had begun to appear, as well as the eruption of a large number of kimberlites related to plate deep subduction (Stern et al., 2016), which indicates that the presence of the typical modern plate tectonic mechanism of global continental cold, deep subduction in the 1.0 Ga period is beyond doubt (Brown et al., 2020).

Due to the combined effects of continental weathering, biological processes and post-glacial denudation weathering, the subducted oceanic crustal plate in the Paleoproterozoic carries much thicker sediments than in the Archean. The significantly reduced ε_{Hf} isotope and increased oxygen isotopes of worldwide detrital zircon in 2.3–2.1 Ga indicate the increased contribution of recycled sediments (Dhuime et al., 2012; Spencer et al., 2017) (Fig. 3). This massive amount of sediment can act as a lubricant in the subduction zone, thus facilitating the plate becoming steadily subducted into the deep mantle (Stephan and Brown, 2019), which was also been verified by the 2.1 Ga global alkaline magma (Liu et al., 2019a). A peak period of continental large igneous provinces occurs at about 1.8 Ga (Li et al., 2019). Numerical simulation results show that the possible formation of many mantle plumes related to large igneous provinces was caused by the subduction of plates disturbing the bottom of the convective mantle, the transition zone and even the core–mantle boundary (Steinberger and Torsvik, 2012). Therefore, the peak of the 1.8 Ga large igneous province may be formed by deep mantle disturbances caused by cold, deep subduction of the Paleoproterozoic oceanic crust (Stephan and Brown, 2019). From the evidence of rock samples, the thermal structure of the subduction zone,

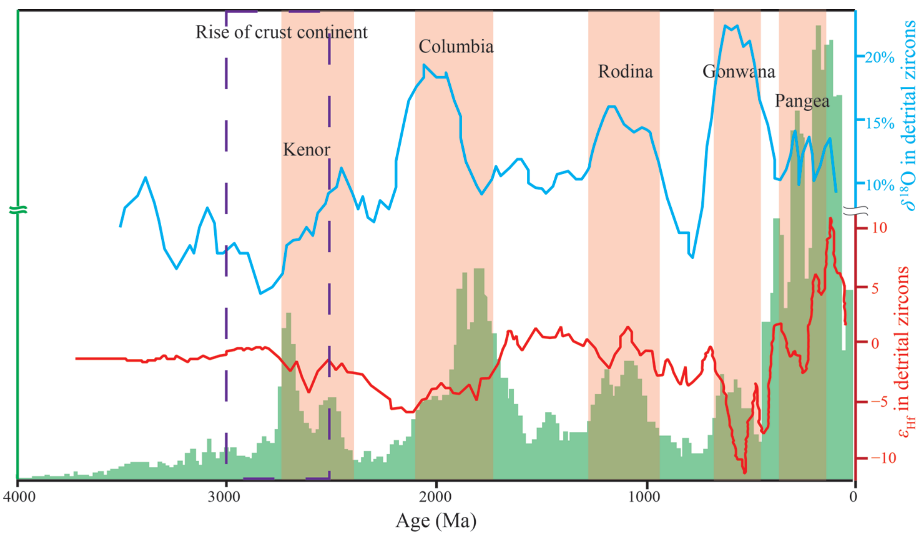

Fig. 3. Hf and O isotopes of detrital zircon and igneous zircon distribution in geological history (Cawood et al., 2013; Spencer et al., 2017).

The blue line shows the $\delta^{18}O$ trend in detrital zircon and the red line shows the ε_{Hf} trend in detrital zircon. The purple dashed outlined box represents the rising process of the continent (Bindeman et al., 2018; Liu and He, 2021).

the ‘lubrication’ of the massive overlying sediments, the isotopic records of significant recycling and the response of the deep mantle, the Paleoproterozoic instead of the Archean has the first global cold, deep subduction (Stephan and Brown, 2019). Thus, the Archean subduction into the deep mantle is not comparable to the Paleoproterozoic orogenic event in terms of scale and depth. Paleoproterozoic cold, deep subduction may be the earliest global event that brought surface materials into the deep mantle for recycling and had a far-reaching impact on Earth’s long-term evolution. Although modern subduction was suspended during the ‘boring billion’, there is no doubt that modern subduction appeared again in the Neoproterozoic and operates to the present. Modern -style plate tectonics in the Neoproterozoic is characterized by the global operation of both cold subduction and hot rifting along narrow plate boundaries and weak mobile belts. Blueschist was discovered in Aksu dating to 700–800 Ma (Xia et al., 2019) and eclogite can be found close to the Neoproterozoic orogenic belt. With decreasing mantle potential temperature, carbon was easily subducted into the deep mantle by cold subduction in the Neoproterozoic.

4 The Coupling of Depth and Period of Carbon in Deep Subduction

4.1 Carbon release from the arc

After a period of a tectonic-magmatic lull during 2.3–2.2 Ga, the eruption period of magma began to appear from 2.2 Ga, which was reflected in the sudden emergence of a large number of magmatic zircons in different Paleoproterozoic orogenic belts, representing intense island arc magmatic activity during subduction (Spencer et al., 2018). Island arc magma is an important method of carbon release. Metamorphic decarbonation and dissolution decarbonation of carbon-bearing sediments in the subduction zone occurred in front of, under and behind the arc, which separated carbon from the plate and released it back into the atmosphere through island arc magma (Mason et al., 2017; Cui et al., 2021). The large amount of carbon dioxide emitted by island arc magma may be the main driving force to end the Makganyene ice age (McKenzie et al., 2016). Although carbon dioxide was released briefly during this period, the intense weathering after the end of the ice age could keep it relatively stable. Due to the high potential temperature of the mantle in the Archean, all sedimentary carbonates and amounts of carbon in altered ocean crust (AOC) were removed during subduction (Dasgupta, 2013). Although some of the carbon could be released from the island arc in the form of carbon dioxide during Paleoproterozoic subduction, more carbon-bearing sediments would continue to migrate to the deep mantle with AOC, which is reflected in the significant reduction of carbon dioxide partial pressure in the Paleoproterozoic atmosphere (Table 1).

4.2 Carbon released from carbonatite and kimberlite

The first appearance of Archean kimberlites and carbonatites may be related to the melting and release of melts after the delamination of the thick Archean lithospheric mantle at 2.7 Ga, likely having nothing to do with the subduction process (Kopylova et al., 2011). This is consistent with the thinning of the late Archean lithosphere, as obtained from big data statistical analysis (Keller and Schoene, 2012). Due to the high Archean temperatures, the deep magma was still dominated by komatiite and high-magnesium magma. Until the temperature dropped continuously for about 2 Ga, carbonatites and kimberlites reflected the nature of the continental deep carbonated lithosphere (Tappe et al., 2018). Conversely, the Archean mantle is highly reductive and CO_2 melts are difficult to preserve to form a large number of carbonatite melts in the deep parts of the Archean high-temperature and highly reductive mantle (Aulbach and Stagno, 2016).

Table 1 CO_2 content in the Archean and Proterozoic Eons

	Content	Time	References
CO_2	0.03–0.15 bar	2.77 Ga	Catling and Zahnle, 2020
	0.02–0.75 bar	2.75 Ga	Catling and Zahnle, 2020
	0.003–0.015 bar	2.69 Ga	Catling and Zahnle, 2020
	0.05–0.15 bar	2.46 Ga	Catling and Zahnle, 2020
	<0.8 bar	3.8–2.4 Ga	Catling and Zahnle, 2020
	<4%	Late Archean	Catling, 2013
	<30 mbar	Late Archean	Charnay et al., 2020
	20–140 mbar	Late Archean	Lehmer et al., 2020
	2–30 PAL	1.4 Ga	Crockford et al., 2018
	<0.4%	Mesoproterozoic	Catling, 2013
CH_4	>20 ppmv	>2.4 Ga	Catling and Zahnle, 2020
	>5000 ppmv	3.5 Ga	Catling and Zahnle, 2020
	10^3 ppmv	Late Archean	Catling, 2013
	10^2 ppmv	Mesoproterozoic	Catling, 2013

Note: PAL = 280 p.p.m. CO_2.

Recent studies have revealed that in the past 1.0 Ga, the thickness of the craton had been thinned by as much as 150 km, which indicates that the Paleoproterozoic craton was thick and the thinning of the craton might be related to the deep subduction of the carbonated oceanic crust (Sun and Dasgupta, 2020). According to the evolution of mantle potential temperature, the 2.1 Ga mantle potential temperature was 160–175°C higher than the present. At this temperature, the plates continued to subduct into the deep mantle (Liu et al., 2019a), providing volatiles such as CO_2 and H_2O for the mantle source of kimberlite and carbonatite. According to the *P-T* conditions of the global subduction zone, it was previously accepted that a large number of kimberlites after 1.0 Ga indicated the beginning of modern plate tectonics (Stern et al., 2016; Zheng and Zhao, 2020). However, recent studies showed that the global metamorphic *P-T* conditions in the 2.0 Ga period were lower than those in the 1.0 Ga period (Brown et al., 2020) (Fig. 2). Continental rifts and cold subduction are the determinants of kimberlite magma generation (Tappe et al., 2018). The carbonatites and kimberlites distributed in the 2.1–1.8 Ga orogenic belts do not possess the characteristics of continental rifting, but of the eruption of carbonatites and kimberlites caused by cold, deep subduction that created the linear distribution of carbonatite and kimberlite in North America (Duke et al., 2014a). 1.8 Ga carbonatite has obvious $\delta^{11}B$ isotope characteristics of $\delta^{11}B > -4‰$, which may also imply the participation of crust-derived sediments, caused by subduction in the source area (Hulett et al., 2016).

It has been reported that many diamond, kimberlite and K-Mg lamprophyre source areas are related to subduction. The Venetia kimberlite that erupted at 0.5 Ga and the Premier kimberlite that erupted at 1.2 Ga in the Kaapvaal craton of South Africa contain diamonds formed at 2.0 Ga (Richardson and Shirey, 2008; Richardson et al., 2009). Most of the diamond-bearing eclogite inclusions were formed later than 2.2 Ga (Shirey and Richardson, 2011). The Jericho kimberlite that erupted in 173 Ma contains 2.0–2.7 Ga diamonds with obvious organic carbon characteristics (Smart et al., 2011). The source area of the Gaussberg K-Mg lamprophyre that erupted at 56 ka in Antarctica shows the characteristics of 2.0–3.0 Ga sediments. The extremely thick cratonic lithospheric mantle formed by 3.0–2.5 Ga also provides favorable conditions for diamond formation (Perchuk et al., 2020). Among them, the diamond ages of the Siberia Craton and the Kaapvaal craton are mostly 2.1–1.8 Ga. Although the diamond age of the Kimberley craton in Western Australia is about 1.58 Ga, it may be related to the 1.8 Ga oceanic crust subduction and the subsequent formation and cratonization of the King Leopold Orogen (Smit et al., 2010).

4.3 Carbon released from OIB

It is generally believed that HIMU (high 'μ', where $\mu = {}^{238}U/{}^{204}Pb$) has the lowest SiO_2 content, the highest CaO/Al_2O_3 and the lowest ${}^{87}Sr/{}^{86}Sr$ content (Jackson and Dasgupta, 2008) (Fig. 4). The existence of carbonate inclusions in HIMU peridotite phenocrysts and trace elements demonstrated that the source area of HIMU must have the participation of carbonate (Weiss et al., 2016), which not only leads to the production of carbonatite metasomatic melt, but also promotes the melting of carbonated eclogite/pyroxenite below the peridotite solidus to generate the melt of the HIMU end component (Jackson and Dasgupta, 2008). There is a slight debate about whether its source area is carbonated eclogite, carbonated peridotite, or just carbonate rock, with different opinions existing regarding the age of its source area. According to the S-MIF characteristics in the HIMU basalt, the HIMU source is believed to be caused by subduction prior to the GOE (Cabral et al., 2013). However, a number of lines of evidence suggest that the S-MIF of sediments disappeared in 2.2 Ga instead of 2.5 Ga (Poulton et al., 2021). Through the two-stage model age, it is considered that the La Palma basalt source with HIMU characteristics was formed at 1.92 Ga (Andersen et al., 2015). Sr-Nd-Pb-Hf and other isotopic means show that the source area of the St. Helena alkaline basalt with HIMU characteristics remains 2.8–1.2 Ga in the mantle (Kawabata et al., 2011). According to the K/U ratio of OIB, the required deep source area should be less than 2.2 Ga (Nielsen, 2010). 2.0–3.5 Ga end element composition is required, based on the Hf-Nd-Pb isotopes of OIB basalt on Mangaia Island (Nebel et al., 2013). The study of the Os-Nd-Pb-Hf isotopes of the HIMU basalt in the Cook-

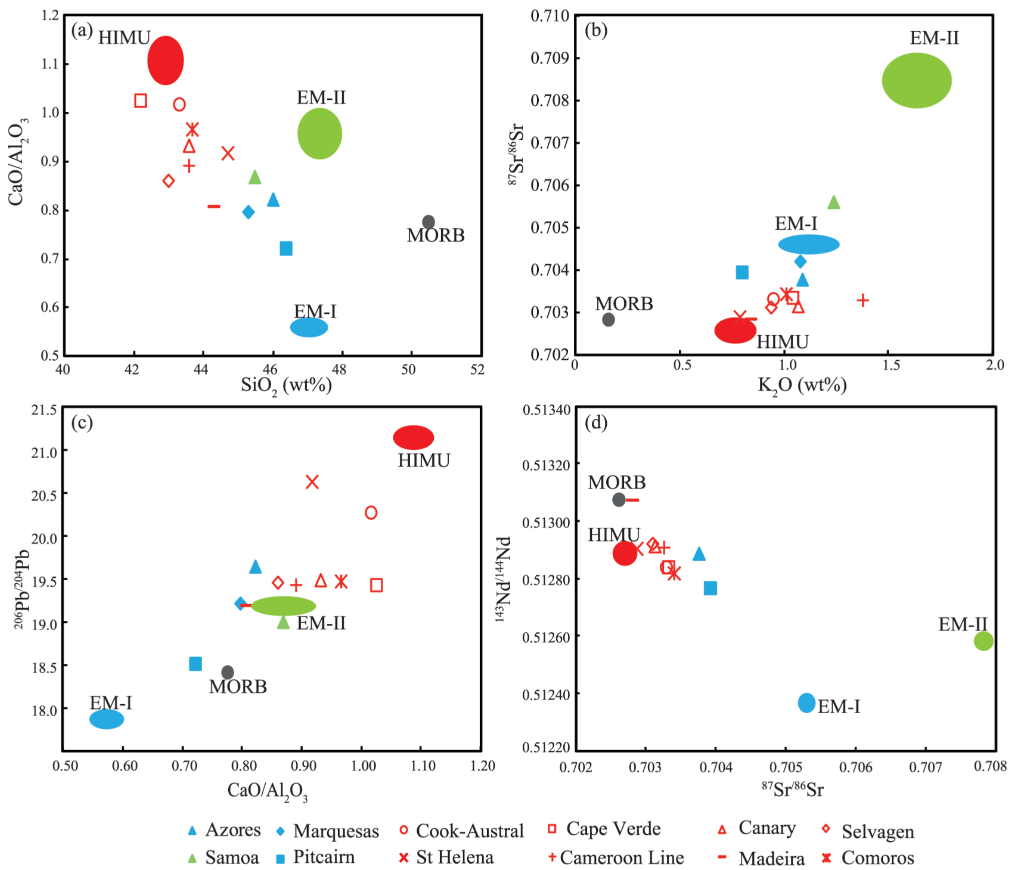

Fig. 4. Geochemical characteristics of HIMU, EM-I, EM-II and MORB with representative locations.
Data were downloaded from the GEOROC database (https://georoc.eu/).

Austral island chain suggests that its source region was formed between 2.0 Ga and 3.0 Ga (Hanyu et al., 2011). The mantle thermal structure and high magnesium andesite indicate that ocean crust plate trapped in the mantle can produce components with HIMU characteristics after 2.5–1.7 Ga (Kimura et al., 2016).

The carbonated AOC is characterized by high U, due to the similar atomic properties of Th and U, which are generally less differentiated in the system. In an oxygen-rich weathering environment, U changes from insoluble U^{4+} to soluble U^{6+}, while Th only has Th^{4+}, which is insoluble in water. Weathering in the aerobic environment induces the differentiation of U and Th, the great oxidation event of 2.33 Ga providing just such an oxygen-rich weathering environment, which greatly reduced the Th/U ratio in river water and seawater (Andersson et al., 1995). After aerobic weathering, U^{6+} mainly exists in water as a steady-state and water-soluble uranyl carbonate complex $[UO_2(CO_3)_3^{4-}]$ (Liu et al., 2019b). The preexisting form of U in the ocean is accompanied by carbonate. In the formation of AOC, a process of ocean crust carbonation, uranium enters AOC with a large amount of carbonate compared with thorium, resulting in a significant reduction in the Th/U ratio. According to ocean-drilling cores, the average Th/U of the upper and middle oceanic crust of AOC can be as low as 0.33 (Staudigel et al., 1996), which is far lower than that of MORB (2.5–2.7). The distribution coefficients of Th and U are similar to the activity in water, making the volcanic rocks formed by the melting of the mantle wedge have slightly similar characteristics of low Th/U, so that more Th and U will enter the deep mantle with the characteristics of low Th/U (Liu et al., 2019b). This low Th/U feature is reflected in many OIBs with HIMU and EM end elements, including Hawaii, Iceland, French Polynesian islands and other deep mantle sources. These OIBs have an ancient (~2 Ga) provenance and the low Th/U feature of the provenance might be affected by the GOE (Andersen et al., 2015). However, U is enriched in sediments due to the valence change of the great oxidation event, while there is no obvious change in Pb, resulting in HIMU characteristics. Similarly, the S-MIF in Mangaia and Cook Islands basalts with HIMU characteristics were previously considered to be caused by Archean subduction (Cabral et al., 2013), though the Archean described in the previous section cannot favor deep subduction. Recent studies have offered more evidence that the source area of HIMU is located in the transition zone (Mazza et al., 2019; Huang et al., 2020), combined with the chemical characteristics of HIMU and EM. Therefore, the source area of Mangaia and Cook Islands basalts might also be the Paleoproterozoic ocean crust with carbonate rocks.

5 The Implications for the Evolution of a Habitable Earth

In the Archean, the atmosphere was full of CO_2 and CH_4. With crustal evolution, continental thickening and uplift made weathering and surface erosion easy, especially at the end of 'snowball Earth', consuming much atmospheric CO_2. During the Paleoproterozoic and Neoproterozoic, intense weathering and surface erosion not only brought nutrients into the ocean and promoted prokaryotes to produce more oxygen, but also promoted sediment deposition, which is helpful for modern subduction. The CO_2 and CH_4 content of the atmosphere declined for a long time, implying more carbon was deposited in sediments and subducted into the deep mantle than before. In the Archean and the short-term carbon cycle (<10 Ma), carbon was released from arcs. Differing from the Archean carbon cycle, which was limited to Earth's surface, in the Paleoproterozoic and Neoproterozoic modern subduction could effectively carry massive carbon into the deep mantle over the long term (from 100 Ma to 2 Ga). Carbon was subducted into the deep mantle then contributed to carbonatite and kimberlite exposed in the Paleoproterozoic and the Neoproterozoic orogenic belt. Carbon-bearing melts reacted with the mantle, forming a large number of diamonds that exist in the mantle root of the ancient craton lithosphere and returned to the ground for several hundred to a billion years. The deep lithosphere delamination metasomatized by carbonatite or the carbon-rich ocean crust stagnant in the transition zone might be the sources of ocean island basalt featuring extreme HIMU (Fig. 5). HIMU type OIB indicates carbon stored in the deep mantle and returned into the atmosphere up to almost 2 billion years later (Fig. 6).

The effective Paleoproterozoic silicate weathering, carbon sequestration and the deep carbon cycle on a large time-space scale may have prevented an uncontrolled greenhouse effect on Earth. Venus is also located in the habitable zone of the solar system and may possess the Archean plate subduction caused by mantle plumes (Davaille et al., 2017). Venus is full of greenhouse gases, leading to a 'runaway greenhouse' effect after the solar intensity reaches a certain threshold. The uncontrolled positive feedback mechanism, by which CO_2 and water vapor fill the atmosphere, results in very high temperatures (T = 740 K) and atmospheric pressures (P = 92 bar) (Lapôtre et al., 2020). In the Paleoproterozoic, when Earth's solar brightness was only 70%–75% compared to now (Feulner, 2012), the CO_2 atmospheric partial pressure might have been between 0.05–0.15 bar or even higher (Catling and Zahnle, 2020). The model predicts that, under current sunlight intensity, 100 times the levels of CO_2 (30000 ppmv ≈ 0.03 bar) can cause the uncontrollable greenhouse effect (Goldblatt et al., 2013). Due to the effective operation of carbon storage and deep subduction in the Paleoproterozoic, a runaway greenhouse effect was not triggered on Earth, unlike on Venus. Unlike Mars, carbon stored in different depths slowly and continuously released CO_2 into the atmosphere, inhibiting the ice age and creating the necessary conditions for liquid water. Oceanic liquid water continues to exist on the surface of Earth, which is necessary for the formation and evolution of life. As for the Neoproterozoic, modern subduction increasingly brought carbon into the deep mantle. The deep carbon cycle process in the Paleoproterozoic and Neoproterozoic and the negative feedback regulatory mechanism not only ensured the emergence of liquid water on Earth's surface for a long time, but also provided the guarantee of a relatively stable

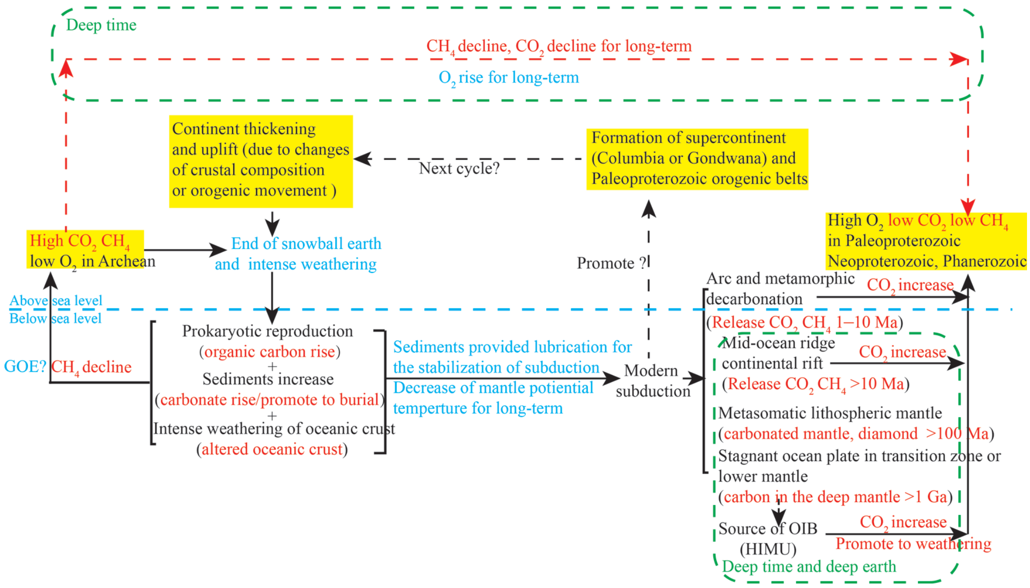

Fig. 5. Carbon cycle model of Paleoproterozoic and Neoproterozoic geological events.
Red text is related to the carbon-bearing process, with blue text relating to weathering and oxygen increase. The blue dashed outlined rectangle represents deep time and the deep earth process. The yellow box shows the states of Earth's continent and atmosphere.

temperature for the evolution of long-term life on Earth (Fig. 5). The Paleoproterozoic and Neoproterozoic carbon cycles promoted the increase of oxygen in the atmosphere, that played a vital role in the evolution of life on Earth. Although the first great oxidation event did not increase the amount of oxygen to current levels, it provided the basis for the Neoproterozoic great oxidation event.

As a carbon buffer with different time scales and reserves, the mantle was fueled with carbon for the first time in the Paleoproterozoic deep subduction and the second time in the Neoproterozoic, up to the present. To date, the mantle is still playing a role in regulating the distribution of carbon by releasing carbon dioxide. The carbon deep cycle is not only the complete exchange of material and energy processes of different earth spheres linked by carbon, but also promotes the evolution of the habitable Earth (Fig. 6).

Acknowledgments

This study was funded by the National Key Research and Development Program of China (Grant No. 2019YFA0708501). We give our great thanks to two anonymous reviewers for their kind and helpful suggestions and comments on the first version of this paper.

Manuscript received Oct. 31, 2022
accepted Feb. 01, 2023
associate EIC: FANG Xiang
edited by Jeffery J. LISTON and GUO Xianqing

References

Alcott, L.J., Mills, B.J.W., and Poulton, S.W., 2019. Stepwise Earth oxygenation is an inherent property of global biogeochemical cycling. Science, 366(6471): 1333–1337.

Andersen, M.B., Elliott, T., Freymuth, H., Sims, K.W.W., Niu, Y., and Kelley, K.A., 2015. The terrestrial uranium isotope cycle. Nature, 517(7534): 356–359.

Andersson, P.S., Wasserburg, G.J., Chen, J.H., Papanastassiou, D.A., and Ingri, J., 1995. ^{238}U-^{234}U and ^{232}Th-^{230}Th in the Baltic Sea and in river water. Earth and Planetary Science Letters, 130(1–4): 217–234.

Aulbach, S., and Stagno, V., 2016. Evidence for a reducing Archean ambient mantle and its effects on the carbon cycle. Geology, 44(9): 751–754.

Baldwin, J.A., Bowring, S.A., Williams, M.L., and Williams, I.S., 2004. Eclogites of the Snowbird tectonic zone: Petrological and U-Pb geochronological evidence for Paleoproterozoic high-pressure metamorphism in the western Canadian Shield. Contributions to Mineralogy and Petrology, 147(5): 528–548.

Bindeman, I.N., Zakharov, D.O., Palandri, J., Greber, N.D., Dauphas, N., Retallack, G.J., Hofmann, A., Lackey, J.S., and Bekker, A., 2018. Rapid emergence of subaerial landmasses and onset of a modern hydrologic cycle 2.5 billion years ago. Nature, 557(7706): 545–548.

Boniface, N., Schenk, V., and Appel, P., 2012. Paleoproterozoic eclogites of MORB-type chemistry and three Proterozoic orogenic cycles in the Ubendian Belt (Tanzania): Evidence from monazite and zircon geochronology, and geochemistry. Precambrian Research, 192–195(1): 16–33.

Brown, M., and Johnson, T., 2018. Secular change in metamorphism and the onset of global plate tectonics. American Mineralogist, 103(2): 181–196.

Brown, M., Kirkland, C.L., and Johnson, T.E., 2020. Evolution of geodynamics since the Archean: Significant change at the dawn of the Phanerozoic. Geology, 48(5): 488–492.

Cabral, R.A., Jackson, M.G., Rose-Koga, E.F., Koga, K.T., Whitehouse, M.J., Antonelli, M.A., Farquhar, J., Day, J.M.D., and Hauri, E.H., 2013. Anomalous sulphur isotopes in plume lavas reveal deep mantle storage of Archaean crust. Nature, 496(7446): 490–493.

Campbell, I.H., and Allen, C.M., 2008. Formation of supercontinents linked to increases in atmospheric oxygen. Nature Geoscience, 1(8): 554–558.

Catling, D.C., 2013. The Great Oxidation Event Transition. Treatise on Geochemistry: Second Edition. Elsevier, 6: 177–195.

Catling, D.C., and Zahnle, K.J., 2020. The Archean atmosphere. Science Advances, 6: eaax1420.

Cawood, P.A., Hawkesworth, C.J., and Dhuime, B., 2013. The continental record and the generation of continental crust. Bulletin of the Geological Society of America, 125(1–2): 14–32.

Charnay, B., Wolf, E.T., Marty, B., and Forget, F., 2020. Is the

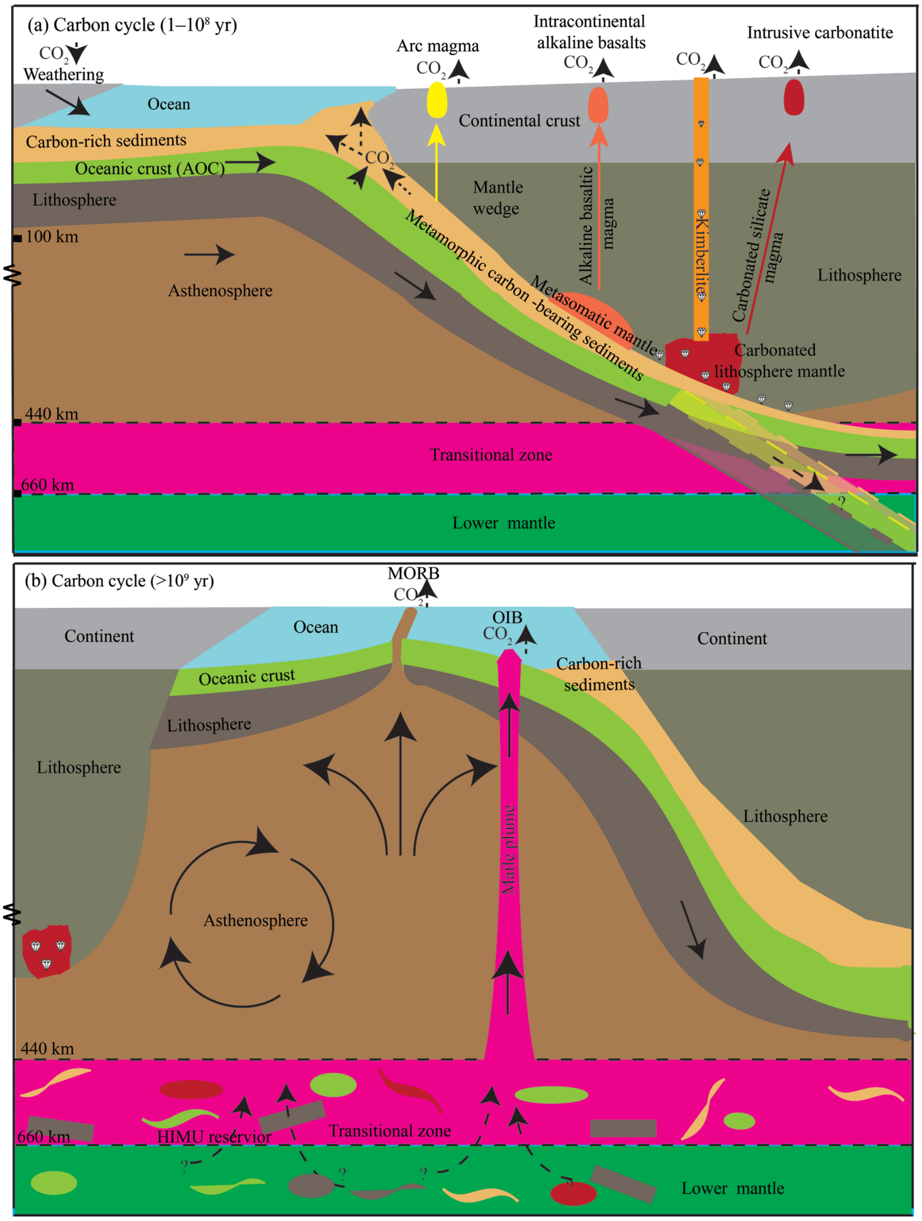

Fig. 6. Diagram showing different scales of the carbon cycle.
The upper picture represents carbon-bearing materials subducting in the Paleoproterozoic or Neoproterozoic and the subsequent release of CO_2 from different depths in 1–10^8 yr. The lower picture represents carbon that was subducted into the deep mantle billions of years ago, being released from OIB and MORB or stored in the deep mantle.

Faint Young Sun Problem for Earth Solved? Space Science Reviews, 216(5): 90.
Crockford, P.W., Hayles, J.A., Bao, H., Planavsky, N.J., Bekker, A., Fralick, P.W., Halverson, G.P., Bui, T.H., Peng, Y., and Wing, B.A., 2018. Triple oxygen isotope evidence for limited mid-Proterozoic primary productivity. Nature, 559(7715): 613–616.
Cui, Y., Li, M.S., Van Soelen, Elsbeth E., Peterse, Francien., Kürschner, and Wolfram M., 2021. Massive and rapid predominantly volcanic CO_2 emission during the end-Permian mass extinction. Proceedings of the National Academy of Sciences of the United States of America, 118(37): e2014701118.
Dasgupta, R., 2013. Ingassing, storage, and outgassing of terrestrial carbon through geologic time. Reviews in Mineralogy and Geochemistry, 75: 183–229.
Dasgupta, R., and Hirschmann, M.M., 2010. The deep carbon cycle and melting in Earth's interior. Earth and Planetary Science Letters, 298(1–2): 1–13.
Davaille, A., Smrekar, S.E., and Tomlinson, S., 2017. Experimental and observational evidence for plume-induced subduction on Venus. Nature Geoscience, 10(5): 349–355.
Dhuime, B., Hawkesworth, C.J., Cawood, P.A., and Storey, C.D., 2012. A change in the geodynamics of continental growth 3 billion years ago. Science, 335(6074): 1334–1336.
Dhuime, B., Wuestefeld, A., and Hawkesworth, C.J., 2015. Emergence of modern continental crust about 3 billion years ago. Nature Geoscience, 8(7): 552–555.
Duke, G.I., Carlson, R.W., Frost, C.D., Hearn, B.C., and Eby, G.N., 2014. Continent-scale linearity of kimberlite-carbonatite magmatism, mid-continent North America. Earth and Planetary Science Letters, 403: 1–14.
Duncan, M.S., and Dasgupta, R., 2017. Rise of Earth's atmospheric oxygen controlled by efficient subduction of organic carbon. Nature Geoscience, 10(5): 387–392.
Eguchi, J., Seales, J., and Dasgupta, R., 2020. Great Oxidation

and Lomagundi events linked by deep cycling and enhanced degassing of carbon. Nature Geoscience, 13(1): 71–76.

Farquhar, J., Bao, H., and Thiemens, M., 2000. Atmospheric influence of Earth's earliest sulfur cycle. Science, 289(5480): 756–758.

Feulner, G., 2012. The faint young Sun problem. Reviews of Geophysics, 50: RG2006.

François, C., Debaille, V., Paquette, J.L., Baudet, D., and Javaux, E.J., 2018. The earliest evidence for modern-style plate tectonics recorded by HP-LT metamorphism in the Paleoproterozoic of the Democratic Republic of the Congo. Scientific Reports, 8: 15452.

Ganade De Araujo, C.E., Rubatto, D., Hermann, J., Cordani, U.G., Caby, R., and Basei, M.A.S., 2014. Ediacaran 2,500-km -long synchronous deep continental subduction in the West Gondwana Orogen. Nature Communications, 5: 1–8.

Ganne, J., de Andrade, V., Weinberg, R.F., Vidal, O., Dubacq, B., Kagambega, N., Naba, S., Baratoux, L., Jessell, M., and Allibon, J., 2012. Modern-style plate subduction preserved in the Palaeoproterozoic West African craton. Nature Geoscience, 5(1): 60–65.

Glassley, W.E., Korstgård, J.A., Ensen, K.S., and Platou, S.W., 2014. A new UHP metamorphic complex in the ~1.8 Ga Nagssugtoqidian Orogen of west Greenland. American Mineralogist, 99(7): 1315–1334.

Goldblatt, C., Robinson, T.D., Zahnle, K.J., and Crisp, D., 2013. Low simulated radiation limit for runaway greenhouse climates. Nature Geoscience, 6(8): 661–667.

Hanyu, T., Tatsumi, Y., and Kimura, J.I., 2011. Constraints on the origin of the HIMU reservoir from He-Ne-Ar isotope systematics. Earth and Planetary Science Letters, 307(3–4): 377–386.

Hazen, R.M., Bromberg, Y., Downs, R.T., Eleish, A., Falkowski, P.G., Fox, P., Giovannelli, D., Hummer, D.R., Hystad, G., Golden, J.J., Knoll, A.H., Li, C., Liu, C., Moore, E.K., Morrison, S.M., Muscente, A.D., Prabhu, A., Ralph, J., Rucker, M.Y., Runyon, S.E., Warden, L.A., and Zhong, H., 2019. Deep carbon through deep time: Data-driven insights. In: Orcutt, B., Daniel, I., and Dasgupta, R. (eds.), Deep Carbon: Past to Present. Cambridge: Cambridge University Press, 620–652.

Herzberg, C., Condie, K., and Korenaga, J., 2010. Thermal history of the Earth and its petrological expression. Earth and Planetary Science Letters, 292(1–2): 79–88.

Holder, R.M., Viete, D.R., Brown, M., and Johnson, T.E., 2019. Metamorphism and the evolution of plate tectonics. Nature, 572(7769): 378–381.

Hu, Q., Kim, D.Y., Yang, W., Yang, L., Meng, Y., Zhang, L., and Mao, H.K., 2016. FeO_2 and FeOOH under deep lower-mantle conditions and Earth's oxygen-hydrogen cycles. Nature, 534(7606): 241–244.

Huang, S., Tschauner, O., Yang, S., Humayun, M., Liu, W., Gilbert Corder, S.N., Bechtel, H.A., and Tischler, J., 2020. HIMU geochemical signature originating from the transition zone. Earth and Planetary Science Letters, 542: 116323.

Hulett, S.R.W., Simonetti, A., Rasbury, E.T., and Hemming, N.G., 2016. Recycling of subducted crustal components into carbonatite melts revealed by boron isotopes. Nature Geoscience, 9(12): 904–908.

Husson, J.M., Peters, S.E., 2017. Atmospheric oxygenation driven by unsteady growth of the continental sedimentary reservoir. Earth and Planetary Science Letters, 460: 68–75.

Jackson, M.G., and Dasgupta, R., 2008. Compositions of HIMU, EM1, and EM2 from global trends between radiogenic isotopes and major elements in ocean island basalts. Earth and Planetary Science Letters, 276(1–2): 175–186.

Kawabata, H., Hanyu, T., Chang, Q., Kimura, J.I., Nichols, A.R.L., and Tatsumi, Y., 2011. The petrology and geochemistry of St. Helena alkali basalts: Evaluation of the oceanic crust-recycling model for HIMU OIB. Journal of Petrology, 52(4): 791–838.

Keller, C.B., and Schoene, B., 2012. Statistical geochemistry reveals disruption in secular lithospheric evolution about 2.5 Gyr ago. Nature, 485(7399): 490–493.

Kimura, J.I., Gill, J.B., Skora, S., van Keken, P.E., and Kawabata, H., 2016. Origin of geochemical mantle components: Role of subduction filter. Geochemistry, Geophysics, Geosystems, 17(8): 3289–3325.

Konhauser, K.O., Pecoits, E., Lalonde, S.V., Papineau, D., Nisbet, E.G., Barley, M.E., Arndt, N.T., Zahnle, K., and Kamber, B.S., 2009. Oceanic nickel depletion and a methanogen famine before the Great Oxidation Event. Nature, 458(7239): 750–753.

Kopylova, M.G., Afanasiev, V.P., Bruce, L.F., Thurston, P.C., and Ryder, J., 2011. Metaconglomerate preserves evidence for kimberlite, diamondiferous root and medium grade terrane of a pre-2.7 Ga Southern Superior protocraton. Earth and Planetary Science Letters, 312(1–2): 213–225.

Kump, L.R., and Barley, M.E., 2007. Increased subaerial volcanism and the rise of atmospheric oxygen 2.5 billion years ago. Nature, 448(7157): 1033–1036.

Lapôtre, M.G.A., O'Rourke, J.G., Schaefer, L.K., Siebach, K.L., Spalding, C., Tikoo, S.M., and Wordsworth, R.D., 2020. Probing space to understand Earth. Nature Reviews Earth and Environment, 1(3): 170–181.

Lee, C.T.A., Yeung, L.Y., McKenzie, N.R., Yokoyama, Y., Ozaki, K., and Lenardic, A., 2016. Two-step rise of atmospheric oxygen linked to the growth of continents. Nature Geoscience, 9(6): 417–424.

Lehmer, O.R., Catling, D.C., Buick, R., Brownlee, D.E., and Newport, S., 2020. Atmospheric CO_2 levels from 2.7 billion years ago inferred from micrometeorite oxidation. Science Advances, 6: eaay4644.

Li, X., Zhang, L., Wei, C., Bader, T., and Guo, J., 2023. Cold subduction recorded by the 1.9 Ga Salma eclogite in Belomorian Province (Russia). Earth and Planetary Science Letters, 602: 117930.

Li, Z.X., Mitchell, R.N., Spencer, C.J., Ernst, R., Pisarevsky, S., Kirscher, U., and Murphy, J.B., 2019. Decoding Earth's rhythms: Modulation of supercontinent cycles by longer superocean episodes. Precambrian Research, 323: 1–5.

Liu, C.T., and He, Y.S., 2021. Rise of major subaerial landmasses about 3.0 to 2.7 billion years ago. Geochemical Perspectives Letters, 18: 1–5.

Liu, H., Sun, W.D., Zartman, R., and Tang, M., 2019a. Continuous plate subduction marked by the rise of alkali magmatism 2.1 billion years ago. Nature Communications, 10: 3408.

Liu, H., Zartman, R.E., Ireland, T.R., and Sun, W.D., 2019b. Global atmospheric oxygen variations recorded by Th/U systematics of igneous rocks. Proceedings of the National Academy of Sciences of the United States of America, 116 (38): 18854–18859.

Loose, D., and Schenk, V., 2018. 2.09 Ga old eclogites in the Eburnian-Transamazonian orogen of southern Cameroon: Significance for Palaeoproterozoic plate tectonics. Precambrian Research, 304: 1–11.

Luo, G., Ono, S., Beukes, N.J., Wang, D.T., Xie, S., and Summons, R.E., 2016. Rapid oxygenation of Earth's atmosphere 2.33 billion years ago. Science Advances, 2: e160013.

Lyons, T.W., Reinhard, C.T., and Planavsky, N.J., 2014. The rise of oxygen in Earth's early ocean and atmosphere. Nature, 506 (7488): 307–315.

Mason, E., Edmonds, M., and Turchyn, A.V., 2017. Remobilization of crustal carbon may dominate volcanic arc emissions. Science, 294(6348): 290–294.

Mazza, S.E., Gazel, E., Bizimis, M., Moucha, R., Béguelin, P., Johnson, E.A., McAleer, R.J., and Sobolev, A.V., 2019. Sampling the volatile-rich transition zone beneath Bermuda. Nature, 569(7756): 398–403.

McKenzie, N.R., Horton, B.K., Loomis, S.E., Stockli, D.F., Planavsky, N.J., Lee, C.A., 2016. Continental arc volcanism as the principal driver of icehouse-greenhouse variability. Science, 352(6284): 444–448.

Moller, A., Appel, P., Mezger, K., and Schenk, V., 1995. Evidence for a 2 Ga subduction zone: Eclogites in the Usagaran belt of Tanzania. Geology, 23(12): 1067–1070.

Müller, S., Dziggel, A., Sindern, S., Kokfelt, T.F., Gerdes, A., and Kolb, J., 2018. Age and temperature-time evolution of

retrogressed eclogite-facies rocks in the Paleoproterozoic Nagssugtoqidian Orogen, South-east Greenland: Constrained from U-Pb dating of zircon, monazite, titanite and rutile. Precambrian Research, 314: 468–486.
Nebel, O., Arculus, R.J., van Westrenen, W., Woodhead, J.D., Jenner, F.E., Nebel-Jacobsen, Y.J., Wille, M., and Eggins, S.M., 2013. Coupled Hf-Nd-Pb isotope co-variations of HIMU oceanic island basalts from Mangaia, Cook-Austral islands, suggest an Archean source component in the mantle transition zone. Geochimica et Cosmochimica Acta, 112: 87–101.
Nielsen, S.G., 2010. Potassium and uranium in the upper mantle controlled by Archean oceanic crust recycling. Geology, 38 (8): 683–686.
Palin, R.M., Santosh, M., Cao, W., Li, S.S., Hernández-Uribe, D., and Parsons, A., 2020. Secular change and the onset of plate tectonics on Earth. Earth-Science Reviews, 207: 103172.
Pavlov, A.A., Kasting, J.F., Brown, L.L., Rages, K.A., and Freedman, R., 2000. Greenhouse warming by CH_4 in the atmosphere of early Earth. Journal of Geophysical Research: Planets, 105(E5): 11981–11990.
Penman, D.E., Caves Rugenstein, J.K., Ibarra, D.E., and Winnick, M.J., 2020. Silicate weathering as a feedback and forcing in Earth's climate and carbon cycle. Earth-Science Reviews, 209: 103298.
Perchuk, A.L., Gerya, T.V., Zakharov, V.S., and Griffin, W.L., 2020. Building cratonic keels in Precambrian plate tectonics. Nature, 586(7829): 395–401.
Plank, T., and Manning, C.E., 2019. Subducting carbon. Nature, 574(7778): 343–352.
Poulton, S.W., Bekker, A., Cumming, V.M., Zerkle, A.L., Canfield, D.E., and Johnston, D.T., 2021. A 200-million-year delay in permanent atmospheric oxygenation. Nature, 592 (7853): 232–236.
Richardson, S.H., and Shirey, S.B., 2008. Continental mantle signature of Bushveld magmas and coeval diamonds. Nature, 453(7197): 910–913.
Richardson, S.H., Pöml, P.F., Shirey, S.B., and Harris, J.W., 2009. Age and origin of peridotitic diamonds from Venetia, Limpopo belt, Kaapvaal-Zimbabwe craton. Lithos, 112: 785–792.
Shields, G., and Veizer, J., 2002. Precambrian marine carbonate isotope database: Version 1.1. Geochemistry, Geophysics, Geosystems, 3(6): 1–12.
Shirey, S.B., and Richardson, S.H., 2011. Start of the Wilson cycle at 3 Ga shown by diamonds from subcontinental mantle. Science, 333(6041): 434–436.
Smart, K.A., Chacko, T., Stachel, T., Muehlenbachs, K., Stern, R.A., and Heaman, L.M., 2011. Diamond growth from oxidized carbon sources beneath the Northern Slave Craton, Canada: A δ^{13}C-N study of eclogite-hosted diamonds from the Jericho kimberlite. Geochimica et Cosmochimica Acta, 75 (20): 6027–6047.
Smit, K.V., Shirey, S.B., Richardson, S.H., le Roex, A.P., and Gurney, J.J., 2010. Re-Os isotopic composition of peridotitic sulphide inclusions in diamonds from Ellendale, Australia: Age constraints on Kimberley cratonic lithosphere. Geochimica et Cosmochimica Acta, 74(11): 3292–3306.
Spencer, C.J., Roberts, N.M.W., and Santosh, M., 2017. Growth, destruction, and preservation of Earth's continental crust. Earth-Science Reviews, 172: 87–106.
Spencer, C.J., Murphy, J.B., Kirkland, C.L., Liu, Y., and Mitchell, R.N., 2018. A Palaeoproterozoic tectono-magmatic lull as a potential trigger for the supercontinent cycle. Nature Geoscience, 11(2): 97–101.
Staudigel, H., Plank, T., White, B., and Schmincke, H.U., 1996. Geochemical fluxes during seafloor alteration of the basaltic upper oceanic crust: DSDP Sites 417 and 418. In: Bebout, E.G., Scholl, D.W., Kirby, S.H., and Platt, J.P. (eds.), Subduction: Top to Bottom. Geophysical Monograph Series, 96: 19–38.
Steinberger, B., and Torsvik, T.H., 2012. A geodynamic model of plumes from the margins of Large Low Shear Velocity Provinces. Geochemistry, Geophysics, Geosystems, 13: Q01W09.
Stephan, S.V., and Brown, M., 2019. Surface erosion events controlled the evolution of plate tectonics on Earth. Nature, 570(7759): 52–57.
Stern, R.J., Leybourne, M.I., and Tsujimori, T., 2016. Kimberlites and the start of plate tectonics. Geology, 44(10): 799–802.
Sun, C.G., and Dasgupta, R., 2020. Thermobarometry of CO_2-rich, silica-undersaturated melts constrains cratonic lithosphere thinning through time in areas of kimberlitic magmatism. Earth and Planetary Science Letters, 550: 116549.
Tappe, S., Romer, R.L., Stracke, A., Steenfelt, A., Smart, K.A., Muehlenbachs, K., and Torsvik, T.H., 2017. Sources and mobility of carbonate melts beneath cratons, with implications for deep carbon cycling, metasomatism and rift initiation. Earth and Planetary Science Letters, 466: 152–167.
Tappe, S., Smart, K., Torsvik, T., Massuyeau, M., and de Wit, M., 2018. Geodynamics of kimberlites on a cooling Earth: Clues to plate tectonic evolution and deep volatile cycles. Earth and Planetary Science Letters, 484: 1–14.
Wan, B., Yang, X., Tian, X., Yuan, H., Kirscher, U., and Mitchell, R.N., 2020. Seismological evidence for the earliest global subduction network at 2 Ga ago. Science Advances, 6: eabc5491.
Weiss, Y., Class, C., Goldstein, S.L., and Hanyu, T., 2016. Key new pieces of the HIMU puzzle from olivines and diamond inclusions. Nature, 537(7622): 666–670.
Weller, O.M., and St-Onge, M.R., 2017. Record of modern-style plate tectonics in the Palaeoproterozoic Trans-Hudson orogen. Nature Geoscience, 10(4): 305–311.
Xia, B., Zhang, L.F., Du, Z.X., and Xu, B., 2019. Petrology and age of Precambrian Aksu blueschist, NW China. Precambrian Research, 326: 295–311.
Xu, C., Kynický, J., Song, W., Tao, R., Lü, Z., Li, Y., Yang, Y., Pohanka, M., Galiova, M.V., Zhang, L., and Fei, Y., 2018. Cold deep subduction recorded by remnants of a Paleoproterozoic carbonated slab. Nature Communications, 9: 2790.
Yu, H.L., Zhang, L.F., Wei, C.J., Li, X.L., and Guo, J.H., 2017. Age and *P-T* conditions of the Gridino-type eclogite in the Belomorian Province, Russia. Journal of Metamorphic Geology, 35(8): 855–869.
Zhang, Y., Wei, C., and Chu, H., 2020. Paleoproterozoic oceanic subduction in the North China Craton: Insights from the metamorphic *P-T-t* paths of the Chicheng mélange in the Hongqiyingzi Complex. Precambrian Research, 342: 105671.
Zheng, Y.F., and Zhao, G., 2020. Two styles of plate tectonics in Earth's history. Science Bulletin, 65(4): 329–334.

About the first author

LIU Zhicheng, male, born in 1992 in Shandong Province; Ph.D. candidate at the School of Earth and Space Sciences, Peking University. He is currently engaged in research on the carbon cycle of the Paleoproterozoic and evolution of the habitable Earth. E-mail: 1519988185@qq.com.

About the corresponding author

ZHANG Lifei, male, born in 1963 in Lishu County, Jilin Province; Ph.D. in geology; graduated from Peking University; professor of School of Earth and Space Sciences, Peking University. He is now interested in the study on metamorphic geology and deep carbon cycle in subduction zone. E-mail: lfzhang@pku.edu.cn.